STATISTIC AND KYNETIC MODELS FOR WHEAT GRAINS PYROLYSIS COUPLED WITH VOLATILES REFORMING

Oana Cristina PÂRVULESCU[1], Tănase DOBRE[2],
Radu VASILESCU-MIREA[3], Laurențiu CEATRĂ[4], Gustav IAVORSCHI[5]

Slow pyrolysis of wheat grains coupled with volatiles catalytic reforming was performed in a fixed bed reactor under carbon dioxide atmosphere. This produced a char, pyrolytic oil and incondensable gases. The distribution of these fractions was dependent on variations in heat flux, carbon dioxide superficial velocity and catalyst presence in the bed reforming. A statistical model was used to estimate the influence of these process variables on char mass, oil mass and temperature in various zones of the reactor. A one-stage global reaction kinetic model was selected to predict the process dynamics and its parameters were assessed based on experimental data.

Keywords: pyrolysis, catalytic reforming, factorial experiment, kinetic model

1. Introduction

An important concern in the replacement of conventional energy sources (coal, oil, natural gas) with unconventional ones (biomass, solar, wind, geothermal, hydraulic etc) can be observed in the last years. The conventional energy sources are non-renewable and lead to emissions of pollutant gases (CO_2, CO, CH_4, SO_x, NO_x etc), which are responsible for global warming and acid rain, whereas the unconventional energy sources are renewable, cheap, import free and non-polluting.

The use of vegetal biomass, e.g. wood, agricultural crops (sugar cane, sugar beet, corn, wheat, rice, cassava, soybeans, cotton, millet, willow, Sudan grass, switchgrass, miscanthus), forestry wastes (sawdust, bark), agricultural wastes (leaves, stalks, straws, husks, shells, cobs, stones, bagasse), aquatic plants, algae, for energy purposes is frequent [1-4]. Vegetal materials contain mainly polysaccharides (cellulose, hemicellulose, lignin, starch), monosaccharides,

[1] Research scientist, Chemical Engineering Department, University POLITEHNICA of Bucharest, Romania, e-mail: oana.parvulescu@yahoo.com
[2] Prof., Chemical Engineering Department, University POLITEHNICA of Bucharest, Romania
[3] Eng., National Research and Development Institute for Electrical Engineering ICPE-CA, Bucharest
[4] Eng., Chemical Engineering Department, University POLITEHNICA of Bucharest, Romania
[5] Research scientist, Chemical Engineering Department, University POLITEHNICA of Bucharest, Romania

oligosaccharides, fats, proteins, ash and water. Depending on polysaccharides content, there are lignocellulosic materials, containing generally 31-50% cellulose, 15-29% hemicellulose and 15-30% lignine, as well as starchy materials, having a high amount of starch, e.g. cereal grains (65-80%), cassava roots (70-94%) etc [1-6]. Vegetal biomass can be converted into convenient solid, liquid and gaseous fuels by thermo-chemical and biological conversion technologies.

Vegetal materials pyrolysis, consisting of solid thermal degradation without oxygen, is a promising thermo-chemical conversion route. It is usually performed in the presence of a carrier gas which can be inert (nitrogen, argon) or oxidant (carbon dioxide, steam). Depending of reactor heating rate, β, the pyrolytic process can be slow ($\beta \leq 60$ K/min), rapid (600 K/min$\leq\beta\leq$12000 K/min) or flash ($\beta \geq 60000$ K/min) [1].

When lignocellulosic or starchy materials are pyrolyzed, they degrade into a char (rich non-volatiles solid residue) and volatile products (a mixture of gases and vapours). Pyrolysis gases, usually H_2, CO_2, CO, CH_4, C_2H_6, C_2H_4, and a pyrolytic liquid, containing mainly water, aliphatic and aromatic oxygenated compounds, are obtained by volatiles condensation. The pyrolysis products result from primary reactions of solid material devolatilization, producing char, hydrocarbons, aliphatic and aromatic oxygenated compounds, water, carbon, carbon dioxide and monoxide as well as from secondary reactions of primary products degradation, e.g. dry and wet reforming of generated hydrocarbons and oxygenated compounds [7-15]:

$$C_nH_k + nCO_2 \rightarrow 2nCO + (k/2)H_2$$

$$C_nH_k + 2nH_2O \rightarrow nCO_2 + (2n+k/2)H_2$$

$$C_xH_yO_z + (2x-z)H_2O \rightarrow xCO_2 + (2x+y/2-z)H_2$$

The endothermic reforming reactions are favoured by sufficiently long residence time of pyrolytic volatiles in the reaction medium and they can occur at temperatures higher than 500 ^{0}C or in the presence of a catalyst at lower temperatures [4,8]. Ni catalysts, usually supported on Al_2O_3, MgO, SiO_2, ZrO_2, CeO_2, SiO_2, olivine, dolomite, have frequently been used due to their low price and high catalytic activity [2,7,9-15].

Pyrolysis products distribution depends on various process variables, e.g. reactor heating rate, process temperature, flow rate of carrier gas and vegetal material properties. An increase in volatiles production and a decrease in char amount with *heating rate* increasing were reported [4,16,17]. Referring to the *process temperature* influence, it is obvious that an increase in operation temperature produces a decrease in char yield and an enlargement of volatiles yield. At temperatures lower than 500°C, pyrolytic oil and incondensable gases production increases with temperature increasing, whereas at temperatures higher than 500°C, oil yield decreases as well as gas yield and hydrogen percentage increase with temperature increasing, as effect of an enhancement of thermal

reforming of volatiles produced during the pyrolysis process [4,16-27]. A lower *flow rate* of carrier gas leads to a longer residence time of pyrolytic volatiles in the reaction medium which favours the oil vapours reforming, producing a decrease in oil yield and an enlargement of incondensable gases production [4]. Some researchers reported an insignificant or increasing variation of oil amount as the *flow rate* of carrier gas was diminished [18,26]. This is an effect of a very short residence time of the vapours in the condenser, so that they condense partially due to a high percentage of incondensable gases [26]. *Material chemical pretreatment* with various impregnation agents influences the distribution and composition of pyrolytic oil and gases. Unlike the pyrolysis of non-impregnated materials, a lower oil amount and an important production of hydrogen-rich pyrolytic gases can be obtained starting from a vegetal material impregnated with a nickel nitrate solution [7,12]. Metallic nickel (Ni^0) nanocrystallites are formed into porous vegetal structure during the pyrolysis process, which act as a catalyst and activate the volatiles reforming reactions [12].

The pyrolysis products have various applications. The char is useful as a renewable fuel, activated carbon or catalyst support. The pyrolytic gas and oil can be upgraded to obtain combustibles and chemicals. The pyrolytic gas is an important source of hydrogen, which can be used either as a clean fuel in fuel cells and internal combustion engines or as raw material in chemical industry [9-12,14]. The oil, consisting of more than 300 oxygenated compounds, is corrosive and relatively unstable due to its high level of oxygen [2,13]. Oil catalytic steam reforming on Ni-based catalysts is an effective way to diminish the oil oxygen content as well as to produce a hydrogen-rich syngas at relatively low temperature [2,9-13]. The biomass pyrolysis and pyrolytic oil reforming can occur at different sites, e.g. the pyrolysis can take place near the biomass source, while the oil steam reforming can be conducted near the existing infrastructure for hydrogen or oil use [10,11]. The pyrolysis of vegetal materials impregnated with a nickel nitrate solution leads to an *in situ* upgrading of pyrolitic volatiles, producing a decrease in oil oxygen content and an increase in gas hydrogen proportion due to an enhancement of volatiles reforming in the presence of nickel catalyst [12].

The pyrolysis of wheat and corn grains impregnated with nickel nitrate solutions, where both the cereal grains pyrolysis and volatiles catalytic reforming were performed in the same fixed bed in a tubular reactor, was experimentally investigated and modelled in our previous papers [28-31]. The present paper focuses on the qualitative and quantitative characterization of slow pyrolysis of wheat grains in a fixed bed coupled with catalytic reforming of pyrolytic volatiles in a fixed reforming bed. The pyrolysis and reforming processes occur in two sections of the same reactor, the volatiles which leave the pyrolysis section being fed into a reforming section. A laboratory set-up was designed and equipped to study the influence of various parameters on process performance and

experimental data were processed by two models. A statistical model was used to link the final values of dependent process variables to the values of independent process variables and a kinetic one was selected to predict the process dynamics.

2. Experimental part

2.1. Materials

Dry whole wheat grains with a mean equivalent spherical diameter of 2.43 mm and a mean particle mass of 0.95 g were employed as vegetal material in the pyrolysis process. A catalytic reforming of pyrolytic volatiles occurred in a reforming bed consisting of activated carbon supported nickel (Ni/AC) particles. In order to asses the catalyst effect, non-catalytic runs, wherein activated carbon (AC) particles were used instead of Ni/AC particles, were conducted. AC and Ni/AC particles with a mean equivalent spherical diameter of 1.75 mm were obtained as char in the slow pyrolysis process of untreated and Ni (II) impregnated corn grains, in our previous researches [30-32].

2.2. Equipment and procedure

The laboratory set-up used to study the vegetal materials pyrolysis was described in our previous studies [28,29,32]. A 350 g sample of wheat grains is introduced in a 38 mm diameter and 500 mm height quartz tubular reactor. A reforming bed consisting of 50 g of AC or Ni/AC is put on this vegetal material bed, the both beds being separated by porous ceramic Raschig rings. Accordingly, the reactor has a pyrolysis section, wherein the pyrolysis of vegetal material occurs, as well as a reforming section, wherein the pyrolytic volatiles reforming takes place. Each reactor section is heated by its own electric resistance with a preset heat flow and the reforming section heating is started 20 minutes prior to the pyrolysis section heating. The carbon dioxide from a cylinder, whose flow is measured by a flow-meter and controlled by a pressure reducer, is fed into the reactor by a pipe, up-flows through the vegetal material fixed bed, then through the reforming fixed bed and it is evacuated with the volatiles obtained during the pyrolysis and reforming processes. The mixture of gases and vapours is cooled in a condenser, producing pyrolytic oil and incondensable gases. The masses of vegetal material and pyrolytic oil, the reactor wall temperature in the pyrolysis section as well as the bed centre temperature in the both reactor sections are recorded and collected by a data acquisition system.

2.3. Experimental variables

The experimental study of vegetal materials pyrolysis coupled with pyrolytic volatiles reforming under carbon dioxide atmosphere was conducted at two values (levels) of process independent variables (factors), i.e. heat flux at the pyrolysis section wall, q_1, heat flux at the reforming section wall, q_2, carbon

dioxide superficial velocity, w, and mean nickel concentration in Ni/AC particles, c_{Ni}. Two sets of 8 experiences were carried out according to a 2^3 factorial plan (Table 1). The first set refers to non-catalytic runs (AC particles, c_{Ni}=0), whereas the second one corresponds to catalytic runs (Ni/AC particles, c_{Ni}=12 %).

Table 1

Process factors levels

Exp	q_1 (W/m^2)	q_2 (W/m^2)	w (m/hr)	c_{Ni} (%)	Exp	q_1 (W/m^2)	q_2 (W/m^2)	w (m/hr)	c_{Ni} (%)
1	4500	5000	2	0	9	4500	5000	2	12
2	4500	5000	4		10	4500	5000	4	
3	4500	8000	2		11	4500	8000	2	
4	4500	8000	4		12	4500	8000	4	
5	7100	5000	2		13	7100	5000	2	
6	7100	5000	4		14	7100	5000	4	
7	7100	8000	2		15	7100	8000	2	
8	7100	8000	4		16	7100	8000	4	

The vegetal material mass, m, pyrolytic oil mass, m_{oil}, reactor wall temperature in the pyrolysis section, t_{w1}, bed centre temperature in the pyrolysis section, t_{c1}, and bed centre temperature in the reforming section, t_{c2}, were continuously recorded as a function of heating time, τ.

3. Results and discussion

3.1. Pyrolysis experimental curves

The curves illustrating the time variation of vegetal material bed mass, m/m_0, given in Fig. 1, and oil mass, m_{oil}/m_0, shown in Fig. 2, have the same shape of bent step. Generally, a decrease in char yield and an enlargement of oil production occur at high values of heat flux at the pyrolysis section wall, q_1, heat flux at the reforming section wall, q_2, and carbon dioxide superficial velocity, w, for the both non-catalytic and catalytic experimental sets. As expected, a decrease in final oil production takes place in catalytic runs due to the catalytic reforming reactions of oil vapours producing low molecular weight gases.

The dynamics of reactor wall temperature in the pyrolysis section, t_{w1}, bed centre temperature in the pyrolysis section, t_{c1}, and bed centre temperature in the reforming section, t_{c2}, plotted in Figs. 3-5, indicate an increase of temperature values at high values of q_1 and q_2, for the both non-catalytic and catalytic experimental sets. Experimental data in Fig. 5 show lower values of bed centre temperature in the reforming section in catalytic runs than in non-catalytic ones, as effect of endothermic reforming reactions. Characteristic curves of mass and temperature dynamics in Figs. 1-5 highlight that the pyrolysis is faster at the high level of heat flux at the pyrolysis section wall, q_1.

Figures 6 and 7 show material mass loss rate, $-\frac{d(m/m_0)}{d\tau}$, depending on a logarithmic mean temperature between the bed centre and reactor wall in the pyrolysis section, t_m, in the both experimental cases. A slight mass loss from the ambient temperature to about 175°C occurs due to the vegetal material moisture removal. Each differential curve has a single relevant peak, emphasizing that the pyrolysis of wheat grains develops intensely in a main stage which can be attributed to the starch degradation. The values of maximum material loss rate, $\left[-\frac{d(m/m_0)}{d\tau}\right]_{peak}$, and of corresponding logarithmic mean temperature, $(t_m)_{peak}$, under various operation conditions, are summarized in Table 2. Tabulated data show that the peak height and the corresponding temperature are greater at the high value of heat flux at the pyrolysis section wall, q_1, in compliance with the data reported in the related literature [33-38].

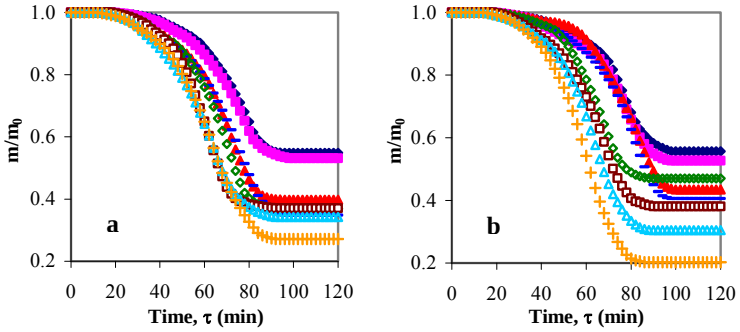

Fig. 1. Time variation of vegetal material mass:
a) non-catalytic runs (♦ exp 1, ■ exp 2, ▲ exp 3, – exp 4, ◊ exp 5, □ exp 6, △ exp 7, + exp 8);
b) catalytic runs (♦ exp 9, ■ exp 10, ▲ exp 11, – exp 12, ◊ exp 13, □ exp 14, △ exp 15, + exp 16).

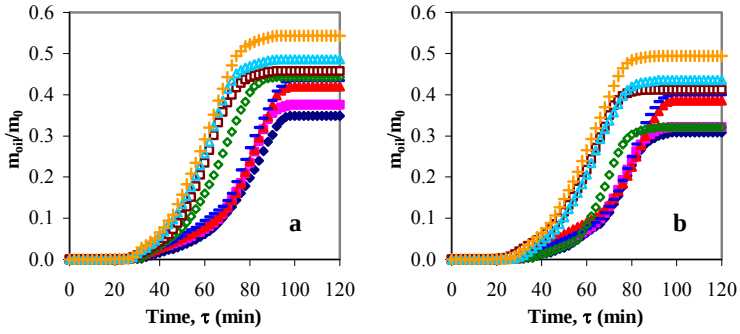

Fig. 2. Time variation of pyrolytic oil mass:
a) non-catalytic runs (♦ exp 1, ■ exp 2, ▲ exp 3, – exp 4, ◊ exp 5, □ exp 6, △ exp 7, + exp 8);
b) catalytic runs (♦ exp 9, ■ exp 10, ▲ exp 11, – exp 12, ◊ exp 13, □ exp 14, △ exp 15, + exp 16).

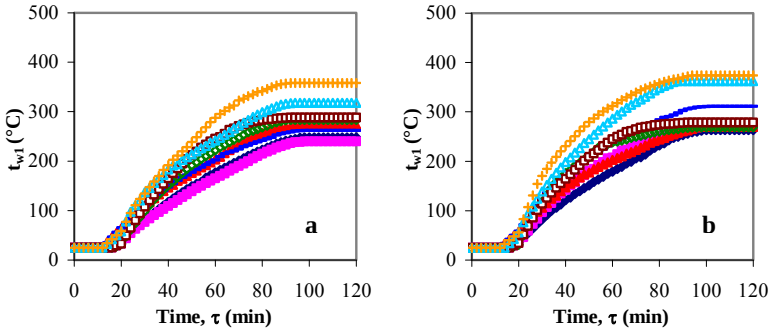

Fig. 3. Time variation of reactor wall temperature in the pyrolysis section:
a) non-catalytic runs (♦ exp 1, ■ exp 2, ▲ exp 3, – exp 4, ◊ exp 5, □ exp 6, △ exp 7, + exp 8);
b) catalytic runs (♦ exp 9, ■ exp 10, ▲ exp 11, – exp 12, ◊ exp 13, □ exp 14, △ exp 15, + exp 16).

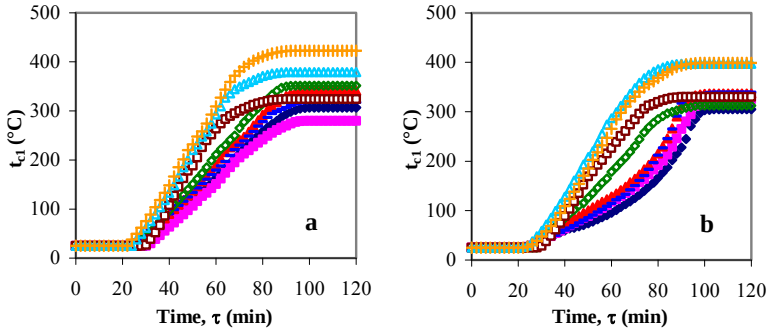

Fig. 4. Time variation of bed centre temperature in the pyrolysis section:
a) non-catalytic runs (♦ exp 1, ■ exp 2, ▲ exp 3, – exp 4, ◊ exp 5, □ exp 6, △ exp 7, + exp 8);
b) catalytic runs (♦ exp 9, ■ exp 10, ▲ exp 11, – exp 12, ◊ exp 13, □ exp 14, △ exp 15, + exp 16).

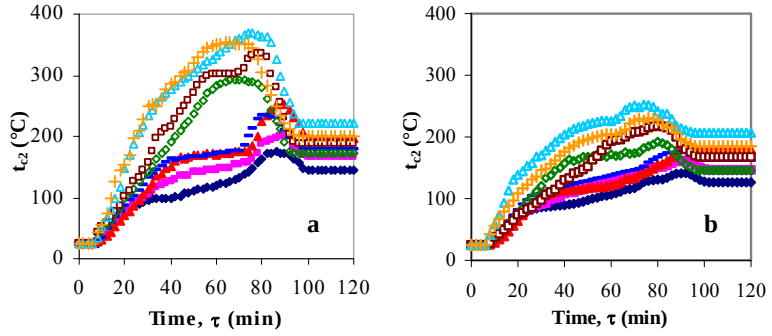

Fig. 5. Time variation of bed centre temperature in the reforming section:
a) non-catalytic runs (♦ exp 1, ■ exp 2, ▲ exp 3, – exp 4, ◊ exp 5, □ exp 6, △ exp 7, + exp 8);
b) catalytic runs (♦ exp 9, ■ exp 10, ▲ exp 11, – exp 12, ◊ exp 13, □ exp 14, △ exp 15, + exp 16).

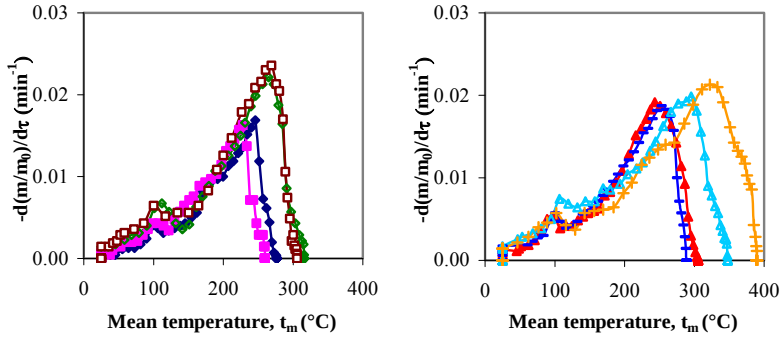

Fig. 6. Mass loss rate versus logarithmic mean temperature in non-catalytic runs (♦ exp 1, ■ exp 2, ▲ exp 3, – exp 4, ◊ exp 5, □ exp 6, △ exp 7, + exp 8).

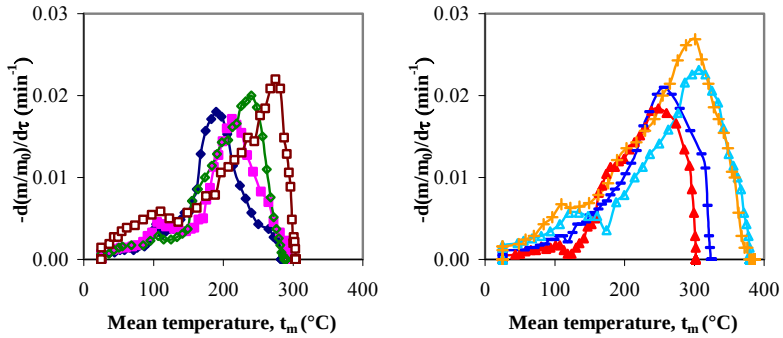

Fig. 7. Mass loss rate versus logarithmic mean temperature in catalytic runs (♦ exp 9, ■ exp 10, ▲ exp 11, – exp 12, ◊ exp 13, □ exp 14, △ exp 15, + exp 16).

Table 2

Maximum material loss rate and corresponding peak temperature

Run	Exp	$\left[-\frac{d(m/m_0)}{d\tau}\right]_{peak}$ (min^{-1})	$(t_m)_{peak}$ (°C)	Run	Exp	$\left[-\frac{d(m/m_0)}{d\tau}\right]_{peak}$ (min^{-1})	$(t_m)_{peak}$ (°C)
non-catalytic	1	0.017	246	catalytic	9	0.018	190
	2	0.016	228		10	0.017	212
	3	0.018	243		11	0.018	249
	4	0.019	253		12	0.021	256
	5	0.022	265		13	0.020	240
	6	0.024	269		14	0.022	275
	7	0.020	296		15	0.023	306
	8	0.021	322		16	0.027	301

3.2. Statistical model

A statistical model based on a 2^3 factorial plan was used to link the final values of dependent process variables (responses) to the values of independent process variables (factors). The vegetal material mass, m, catalytic oil mass, m_{oil}, reactor wall temperature in the pyrolysis section, t_{w1}, bed centre temperature in the pyrolysis section, t_{c1}, and bed centre temperature in the reforming section, t_{c2}, were selected as process responses, whereas the heat flux at the pyrolysis section wall, q_1, heat flux at the reforming section wall, q_2, carbon dioxide superficial velocity, w, and mean nickel concentration in Ni/AC particles, c_{Ni}, were chosen as process factors. Factors dimensionless values were calculated depending on natural values with the following correlations:

$$x_1 = \frac{q_1 - 5800}{1300} \ (1),\ x_2 = \frac{q_2 - 6500}{1500} \ (2),\ x_3 = \frac{w-3}{1} \ (3),\ x_4 = \frac{c_{Ni} - 6}{6} \ (4)$$

Factors dimensionless values as well as responses final values divided by the initial material mass, i.e. $y_1 = \frac{m_f}{m_0}$, $y_2 = \frac{m_{oilf}}{m_0}$, $y_3 = \frac{t_{w1f}}{m_0}$, $y_4 = \frac{t_{c1f}}{m_0}$ and $y_5 = \frac{t_{c2f}}{m_0}$, for non-catalytic and catalytic runs are given in Table 3. The data listed in Table 3 were processed based on the procedure recommended in the case of a 2^3 factorial experiment, for non-catalytic runs (exp 1-exp 8) and catalytic runs (exp 9-exp 16), respectively, and the following correlations were obtained between y_j, j=1…5, and x_i, i=1…3 [39]:

Non-catalyitc runs (x_4=-1):

$$y_1 = 0.398 - 0.059x_1 - 0.058x_2 - 0.017x_3 + 0.026x_1x_2 - 0.001x_1x_3 - 0.013x_2x_3 - 0.006x_1x_2x_3 \quad (5)$$

$$y_2 = 0.438 + 0.044x_1 + 0.032x_2 + 0.014x_3 + 0.004x_1x_3 + 0.007x_2x_3 + 0.004x_1x_2x_3 \quad (6)$$

$$y_3 = 0.811 + 0.080x_1 + 0.054x_2 + 0.009x_3 + 0.021x_1x_2 + 0.023x_1x_3 + 0.012x_2x_3 + 0.013x_1x_2x_3 \quad (7)$$

$$y_4 = 0.972 + 0.083x_1 + 0.071x_2 - 0.012x_3 + 0.020x_1x_2 + 0.024x_1x_3 + 0.027x_2x_3 + 0.024x_1x_2x_3 \quad (8)$$

$$y_5 = 0.524 + 0.035x_1 + 0.046x_2 - 0.003x_3 + 0.001x_1x_2 - 0.002x_1x_3 - 0.027x_2x_3 + 0.001x_1x_2x_3 \quad (9)$$

Catalyitc runs (x_4=1):

$$y_1 = 0.410 - 0.070x_1 - 0.074x_2 - 0.031x_3 - 0.012x_1x_2 - 0.017x_1x_3 - 0.001x_2x_3 - 0.002x_1x_2x_3 \quad (10)$$

$$y_2 = 0.385 + 0.031x_1 + 0.044x_2 + 0.022x_3 + 0.005x_1x_2 + 0.016x_1x_3 - 0.004x_2x_3 - 0.004x_1x_2x_3 \quad (11)$$

$$y_3 = 0.857 + 0.059x_1 + 0.084x_2 + 0.026x_3 + 0.051x_1x_2 - 0.010x_1x_3 + 0.012x_2x_3 - 0.011x_1x_2x_3 \quad (12)$$

$$y_4 = 0.980 + 0.047x_1 + 0.071x_2 + 0.015x_3 + 0.039x_1x_2 - 0.001x_1x_3 - 0.012x_2x_3 + 0.001x_1x_2x_3 \quad (13)$$

$$y_5 = 0.471 + 0.033x_1 + 0.052x_2 + 0.001x_3 + 0.004x_1x_2 - 0.001x_1x_3 - 0.029x_2x_3 - 0.003x_1x_2x_3 \quad (14)$$

Table 3

Experimentation matrix

Run	Exp	x_1	x_2	x_3	x_4	y_1	y_2	y_3 (°C/g)	y_4 (°C/g)	y_5 (°C/g)
non-catalytic	1	-1	-1	-1	-1	0.549	0.349	0.709	0.877	0.417
	2	-1	-1	1	-1	0.531	0.376	0.686	0.800	0.471
	3	-1	1	-1	-1	0.397	0.420	0.779	0.974	0.562
	4	-1	1	1	-1	0.349	0.434	0.749	0.906	0.506
	5	1	-1	-1	-1	0.369	0.443	0.809	1.004	0.491
	6	1	-1	1	-1	0.371	0.457	0.823	0.926	0.534
	7	1	1	-1	-1	0.343	0.486	0.909	1.083	0.636
	8	1	1	1	-1	0.271	0.543	1.023	1.209	0.574
catalytic	9	-1	-1	-1	1	0.557	0.309	0.751	0.873	0.361
	10	-1	-1	1	1	0.527	0.321	0.779	0.929	0.418
	11	-1	1	-1	1	0.434	0.386	0.771	0.962	0.511
	12	-1	1	1	1	0.406	0.400	0.889	0.969	0.463
	13	1	-1	-1	1	0.471	0.321	0.767	0.893	0.417
	14	1	-1	1	1	0.381	0.412	0.796	0.943	0.480
	15	1	1	-1	1	0.305	0.435	1.035	1.134	0.591
	16	1	1	1	1	0.203	0.494	1.068	1.140	0.529

The correlations (5)-(14) and data listed in Table 3 emphasize the following aspects for the both non-catalytic and catalytic experimental sets:

- the final values of solid mass, y_1, are low at superior levels of heat flux at the pyrolysis section wall, x_1, heat flux at the reforming section wall, x_2, and carbon dioxide superficial velocity, x_3;
- the final values of oil mass, y_2, are high at superior levels of x_1, x_2 and x_3;
- the final values of reactor wall temperature in the pyrolysis section, y_3, bed centre temperature in the pyrolysis section, y_4, and bed centre temperature in the reforming section, y_5, are high at superior levels of x_1 and x_2;
- the heat fluxes at the pyrolysis and reforming sections wall, x_1 and x_2, influence significantly the process responses, whereas the carrier gas velocity, x_3, has a less important effect.

To asses the effect of catalytic reforming on the process responses, the data listed in Table 3 were processed for low gas velocity runs (exp 1, 3, 5, 7, 9, 11, 13, 15) and for high gas velocity runs (exp 2, 4, 6, 8, 10, 12, 14, 16). According to the procedure recommended for a 2^3 factorial experiment, the following correlations were obtained between y_j, j=1…5, and x_i, i=1, 2, 4 [39]:

Low gas velocity runs (x_3=-1):

$$y_1 = 0.428 - 0.056x_1 - 0.058x_2 + 0.014x_4 + 0.010x_1x_2 + 0.002x_1x_4 - 0.014x_2x_4 - 0.021x_1x_2x_4 \quad (15)$$

$$y_2 = 0.394 + 0.028x_1 + 0.038x_2 - 0.031x_4 + 0.001x_1x_2 - 0.012x_1x_4 + 0.010x_2x_4 + 0.008x_1x_2x_4 \quad (16)$$

$$y_3 = 0.816 + 0.064x_1 + 0.057x_2 + 0.015x_4 + 0.035x_1x_2 + 0.006x_1x_4 + 0.015x_2x_4 + 0.027x_1x_2x_4 \quad (17)$$

$$y_4 = 0.975 + 0.054x_1 + 0.063x_2 - 0.010x_4 + 0.017x_1x_2 - 0.006x_1x_4 + 0.019x_2x_4 + 0.021x_1x_2x_4 \quad (18)$$

$$y_5 = 0.498 + 0.035x_1 + 0.077x_2 - 0.028x_4 + 0.003x_1x_2 - 0.002x_1x_4 + 0.004x_2x_4 + 0.003x_1x_2x_4 \quad (19)$$

High gas velocity runs (x_3=1):

$$y_1 = 0.380 - 0.073x_1 - 0.073x_2 - 0.001x_4 + 0.003x_1x_2 - 0.014x_1x_4 - 0.002x_2x_4 - 0.017x_1x_2x_4 \quad (20)$$

$$y_2 = 0.430 + 0.047x_1 + 0.038x_2 - 0.023x_4 + 0.004x_1x_2 - 0.001x_1x_4 + 0.002x_2x_4 - 0.003x_1x_2x_4 \quad (21)$$

$$y_3 = 0.852 + 0.076x_1 + 0.081x_2 + 0.031x_4 + 0.037x_1x_2 - 0.027x_1x_4 + 0.015x_2x_4 + 0.003x_1x_2x_4 \quad (22)$$

$$y_4 = 0.978 + 0.077x_1 + 0.078x_2 + 0.017x_4 + 0.042x_1x_2 - 0.031x_1x_4 - 0.019x_2x_4 - 0.003x_1x_2x_4 \quad (23)$$

$$y_5 = 0.497 + 0.032x_1 + 0.021x_2 - 0.024x_4 + 0.001x_1x_2 - 0.002x_1x_2x_4 \quad (24)$$

The correlations (15)-(24) and data listed in Table 3 highlight that the presence of the catalytic reforming bed has an important influence on the final values of oil mass, y_2, and bed centre temperature in the reforming section, y_5. As expected, y_2 and y_5 final values are lower in the presence of Ni/AC reforming bed due to the endothermic catalytic reforming reactions of oil vapours producing low molecular weight gases.

3.3. Kinetic model

A one-stage global reaction kinetic model was selected to predict the conversion process from raw vegetal material to char and volatiles [8,17,33-35,40]. For dynamic data obtained at a constant heating rate, $\beta = \frac{dT_m}{d\tau}$, the decomposition rate can be described by equation [40]:

$$\frac{d\alpha}{d\tau} = (1-\alpha)\frac{A}{\beta}\exp\left(-\frac{E}{RT_m}\right) \quad (25)$$

where the volatiles conversion is expressed as:

$$\alpha = \frac{m_0 - m}{m_0 - m_f} \quad (26)$$

Taking natural logarithms on the both sides of Eq. (25) yields:

$$\ln\left(\frac{1}{1-\alpha}\frac{d\alpha}{d\tau}\right) = \ln\frac{A}{\beta} - \frac{E}{RT_m} \quad (27)$$

The values of pre-exponential factor, A/β, and activation energy, E, depending on the operation conditions were obtained from the intercept and the slope of the straight line given by a plot of $ln\left(\frac{1}{1-\alpha}\frac{d\alpha}{d\tau}\right)$ versus $\frac{1}{T_m}$. Characteristic

values of A/β and E kinetic parameters, which were regressed based on experimental data under various operation conditions, are summarized in Table 4. Table 4 contains also the mean values of heating rate, β, as well as the ranges of temperature, t_m, and conversion, α, wherein the mean values of β were estimated. As can be seen, the pre-exponential factor and activation energy increase with q_1 and q_2 heat fluxes decreasing.

Table 4

Effect of process factors on kinetic parameters

Runs	Exp.	$\beta=dT_m/d\tau$ (K/min)	t_m (°C)	α	A/β (min^{-1})	E (kJ/mole)
non-catalytic	1	3.03	221-257	0.59-0.96	6.34×10^{10}	113.35
	2	3.02	204-234	0.56-0.87	3.79×10^{8}	89.51
	3	3.61	224-281	0.49-0.93	3.44×10^{5}	64.93
	4	3.20	206-275	0.40-0.93	7.98×10^{5}	68.65
	5	3.77	197-309	0.30-0.99	6.36×10^{4}	58.37
	6	3.68	237-285	0.42-0.89	2.23×10^{6}	74.90
	7	3.90	226-334	0.36-0.95	8.98×10^{2}	43.07
	8	5.76	236-351	0.27-0.75	0.71×10^{2}	43.28
catalytic	9	3.38	150-205	0.28-0.79	9.37×10^{6}	70.32
	10	3.07	164-226	0.26-0.79	1.24×10^{7}	75.11
	11	4.27	180-293	0.26-0.93	4.96×10^{3}	46.41
	12	4.28	175-279	0.24-0.83	8.88×10^{3}	49.68
	13	3.57	191-262	0.30-0.92	2.94×10^{5}	62.05
	14	3.81	236-287	0.44-0.85	8.46×10^{5}	71.59
	15	4.76	226-356	0.24-0.90	6.23×10^{2}	43.02
	16	4.97	254-342	0.39-0.88	3.61×10^{2}	39.70

Figures 8 and 9 compare the differential conversion curves predicted by estimated kinetic parameters with the experimental results for non-catalytic and catalytic runs. A good agreement between the experimental and simulated data is proved (errors less than 10 %).

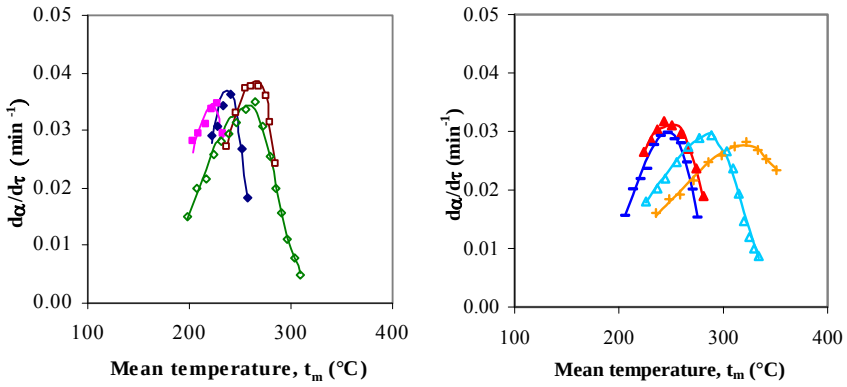

Fig. 8. Experimental (symbols) and predicted (lines) differential conversion curves in non-catalytic runs (♦ exp 1, ■ exp 2, ▲ exp 3, – exp 4, ◊ exp 5, □ exp 6, △ exp 7, + exp 8).

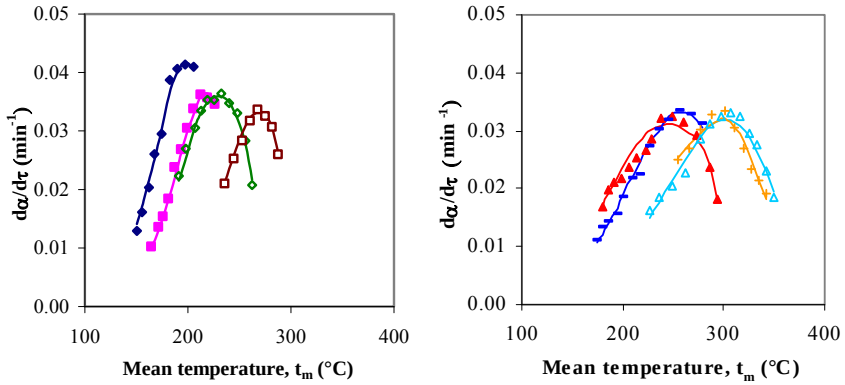

Fig. 9. Experimental (symbols) and predicted (lines) differential conversion curves in catalytic runs (♦ exp 9, ■ exp 10, ▲ exp 11, – exp 12, ◊ exp 13, □ exp 14, △ exp 15, + exp 16).

4. Conclusions

An experimental set-up was designed and scaled-up in order to study the slow pyrolysis of wheat grains coupled with the catalytic reforming of pyrolytic volatiles. The fixed bed pyrolysis and reforming occurred in two sections of the same tubular reactor, the volatiles leaving the pyrolysis section being fed into a reforming section. Carbon dioxide was employed as a carrier agent and a reactant in the both processes. A char, a pyrolytic oil and a gaseous fraction were produced.

A process analysis by 2^3 factorial programming was performed with the factors being the heat flux at the pyrolysis section wall, q_1, heat flux at the reforming section wall, q_2, carbon dioxide superficial velocity, w, and mean nickel concentration in Ni/AC particles, c_{Ni}. A statistical model was used to link the final values of process responses, i.e. char mass, oil mass, reactor wall temperature in the pyrolysis section, bed centre temperature in the pyrolysis and reforming sections, to the factors values. Under the studied conditions, the heat fluxes at the pyrolysis and reforming sections as well as the catalyst presence had a significant effect on the process performances.

A one-stage global reaction kinetic model, whose parameters were estimated based on experimental data, was selected to simulate the process dynamics. The model predicted well the real conditions and it could facilitate the design, scaling-up and operation of fixed bed pyrolysis reactors.

Nomenclature

A/β	pre-exponential factor, min^{-1}
c_{Ni}	mean nickel concentration in Ni/AC particles, %
E	activation energy, kJ/mole

m vegetal material mass, g
m_{oil} pyrolytic oil mass, g
m_0 initial vegetal material mass, g
q heat flux, W/m^2
R gas universal constant, R=8314 J/mole K
t temperature, °C
T absolute temperature, K
w carbon dioxide superficial velocity, m/hr
x_i process dimensionless factor, i=1…4
y_j process final response, j=1…5

Greek letters

α volatiles conversion
β heating rate, $\beta = \frac{dT_m}{d\tau}$, K/min
τ time, min

Subscripts

c fixed bed centre
f final
m logarithmic mean
w reactor wall
0 initial
1 pyrolysis section
2 reforming section

REFERENCES

[1] *M. Balat, M. Balat, E. Kirtay and H. Balat*, "Main routes for the thermo-conversion of biomass into fuels and chemicals. Part 1: Pyrolysis systems", Energ. Convers. Manage., **vol. 50**, 2009, pp. 3147-3157
[2] *D.A. Bulushev and J.R.H. Ross*, "Catalysis for conversion of biomass to fuels via pyrolysis and gasification: A review", Catalysis Today, **vol. 171**, 2011, pp. 1-13
[3] *A. Demirbaş, E. Pehlivan and T. Altun*, "Potential evolution of Turkish agricultural residues as bio-gas, bio-char and bio-oil sources", Int. J. Hydrogen Energ., **vol. 31**, 2006, pp. 613-620
[4] *R. Zanzi*, Pyrolysis of biomass, Dissertation, Royal Institute of Technology, Stockholm, 2001
[5] *R. Lásztity*, Cereal chemistry, Akadémiai Kiadó, Budapest, Hungary, 1999
[6] *E. Nuwamanya, Y. Baguma, N. Emmambux, J. Taylor and R. Patrick,* "Physicochemical and functional characteristics of cassava starch in Ugandan varieties and their progenies", J. Plant Breeding Crop Sci., **vol. 2**, 2010, pp. 1-11
[7] *K. Bru, J. Blin, A. Julbe and G. Volle*, "Pyrolysis of metal impregnated biomass: An innovative catalytic way to produce gas fuel", J. Anal. Appl. Pyrolysis, **vol. 78**, 2007, pp. 291-300
[8] *C. Di Blasi*, "Modeling chemical and physical processes of wood and biomass pyrolysis", Prog. Energy Combust. Sci., **vol. 34**, 2008, pp. 47-90
[9] *L. Garcia, R. French, S. Czernik and E. Chornet*, "Catalytic steam reforming of bio-oils for the production of hydrogen: effects of catalyst composition", Applied Catalysis A: General, **vol. 201**, 2000, pp. 225-239

[10] *P.N. Kechagiopoulos, S.S. Voutetakis, A.A. Lemonidou and I.A. Vasalos*, "Hydrogen production via steam reforming of the aqueous phase of bio-oil in a fixed bed reactor", Energy & Fuels, **vol. 20**, 2006, pp. 2155-2163
[11] *P.N. Kechagiopoulos, S.S. Voutetakis, A.A. Lemonidou and I.A. Vasalos*, "Sustainable hydrogen production via reforming of ethylene glycol using a novel spouted bed reactor", Catalysis Today, vol. 127, 2007, pp. 246-255
[12] *Y. Richardson, J. Blin, G. Volle, J. Motuzas and A. Julbe*, "In situ generation of Ni metal nanoparticles as catalyst for H_2-rich syngas production from biomass gasification", Applied Catalysis A: General, vol. 382, 2010, pp. 220-230
[13] *C. Wu, Y. Yan, T. Li and W. Qi*, "Preparation of hydrogen through catalytic steam reforming of bio-oil", Chinese Journal of Process Engineering, vol. 7, 2007, pp. 1114-1119
[14] *W. Wu, K. Kawamoto and H. Kuramochi*, "Hydrogen-rich synthesis gas production from waste wood via gasification and reforming technology for fuel cell application", J. Mater. Cycles Waste Manag., **vol. 8**, 2006, pp. 70-77
[15] *M.M. Yung, W.S. Jablonski and K.A. Magrini-Bair*, "Review of catalytic conditioning of biomass-derived syngas", Energy & Fuels, **vol. 23**, 2009, pp. 1874-1887
[16] *J.F. Gonzalez, J.M. Encinar, J.L. Canito, E. Sabio and M. Chacon*, "Pyrolysis of cherry stones: energy uses of the different fractions and kinetic study", J. Anal. Appl. Pyrolysis, **vol. 67**, 2003, pp. 165-190
[17] *S. Xiu, Z. Li, B. Li, W. Yi and X. Bai*, "Devolatilization characteristics of biomass at flash heating rate", Fuel, 85, 2006, pp. 664-670
[18] *C. Acikgoz, O. Onay and O.M. Kockar*, "Fast pyrolysis of linseed: product yields and compositions", J. Anal. Appl. Pyrolysis, **vol. 71**, 2004, pp. 417-429
[19] *A. Çağlar and A. Demirbaş*, "Hydrogen rich gas mixture from olive husk via pyrolysis", Energ. Convers. Manage., **vol. 43**, 2002, pp. 109-117
[20] *A. Çağlar and A. Demirbaş*, "Conversion of cotton cocoon shell to hydrogen rich gaseous products by pyrolysis", Energ. Convers. Manage., **vol. 43**, 2002, pp. 489-497
[21] *T. Damartzis, G. Ioannidis and A. Zabaniotou*, "Simulating the behavior of a wire mesh reactor for olive kernel fast pyrolysis", Chem. Eng. J., **vol. 136**, 2008, pp. 320-330
[22] *A. Demirbaş*, "Gaseous products from biomass by pyrolysis and gasification: effects of catalyst on hydrogen yield", Energ. Convers. Manage., **vol. 43**, 2002, pp. 897-909
[23] *A. Demirbaş*, "Partly chemical analysis of liquid fraction of flash pyrolysis products from biomass in the presence of sodium carbonate", Energ. Convers. Manage., **vol. 43**, 2002, pp. 1801-1809
[24] *A. Demirbaş*, "Effect of temperature on pyrolysis products from four nut shells", J. Anal. Appl. Pyrolysis, **vol. 76**, 2006, pp. 285-289
[25] *C. Di Blasi, G. Signorelli, C. Di Russo and G. Rea*, "Product distribution from pyrolysis of wood and agricultural residues", Ind. Eng. Chem. Res., **vol. 38**, 1999, pp. 2216-2224
[26] *M.F. Parihar, M. Kamil, H.B. Goyal, A.K. Gupta and A.K. Bhatnagar*, "An experimental study on pyrolysis of biomass", Trans IChemE, **vol. 85 (B5)**, 2007, pp. 458-465
[27] *A. Zabaniotou and O. Ioannidou*, "Evaluation of utilization of corn stalks for energy and carbon material production by using rapid pyrolysis at high temperature", Fuel, **vol. 87**, 2008, pp. 834-843
[28] *T. Dobre, O.C. Pârvulescu, G. Iavorschi, A. Stoica and M. Stroescu*, "Catalytic effects at pyrolysis of wheat grains impregnated with nickel salts", International Journal of Chemical Reactor Engineering, **vol. 8**, 2010, pp. 1968-1992
[29] *T. Dobre, O.C. Pârvulescu, L. Ceatră, M. Stroescu and G. Iavorschi*, "Catalytic effects at the vegetal materials pyrolysis", in Proceedings of the 6th European Meeting on Chemical Industry and Environment (EMChIE), May 17-19, 2010, Mechelen, Belgium, **vol. 1**, pp. 605-615

[30] *T. Dobre, O.C. Pârvulescu, I. Rodriguez Ramos, L. Ceatră, M. Stroescu, A. Stoica and R. Mirea*, "Global reaction kinetics and enthalpy in slow pyrolysis of vegetal materials", Rev. Chim.-Bucharest, **vol. 63**, 2012, pp. 54-59
[31] T. Dobre, O.C. Pârvulescu, L. Ceatră, M. Stroescu and A. Stoica, 2012, "Fixed bed pyrolysis of untreated and Ni (II) impregnated corn grains: experiment and modelling", U.P.B. Sci. Bull. Series B, 2012, vol. 74, pp. 143-158
[32] O.C. Pârvulescu, T. Dobre, L. Ceatră, G. Iavorschi and R. Mirea, "Characteristics of corn grains pyrolysis in a fixed bed reactor", Rev. Chim.-Bucharest, vol. 62, 2011, pp. 89-94
[33] A. Aboulkas, K. El harfi, A. El bouadili, M. Nadifiyine, M. Benchanaa and A. Mokhlisse, "Pyrolysis kinetics of olive residue/plastic mixtures by non-isothermal thermogravimetry", Fuel Process. Technol., **vol. 90**, 2009, pp. 722-728
[34] *L.S. Guinesi, A.L. da Roz, E. Corradini, L.H.C. Mattoso, E.M. Teixeira and A.A.S. Curvelo*, "Kinetics of thermal degradation applied to starches from different botanical origins by non-isothermal procedures", Thermochim. Acta, **vol. 447**, 2006, pp. 190-196
[35] *S. Hu, A. Jess and M. Xu*, "Kinetic study of Chinese biomass slow pyrolysis: Comparison of different kinetic models", Fuel, **vol. 86**, 2007, pp. 2778-2788
[36] *M. Jeguirim and G. Trouvé*, "Pyrolysis characteristics and kinetics of *Arundo donax* using thermogravimetric analysis", Biores. Technol., **vol. 100**, 2009, pp. 4026-4031
[37] *Z. Li, W. Zhao, B. Meng, C. Liu, Q. Zhu and G. Zhao*, "Kinetic study of corn straw pyrolysis: Comparison of two different three-pseudocomponent models", Biores. Technol., **vol. 99**, 2008, pp. 7616-7622
[38] *F. Yu, R. Ruan and P. Steele*, "Consecutive reaction model for the pyrolysis of corn cob", Trans. ASABE, **vol. 51**, 2008, pp. 1023-1028
[39] *T. Dobre and J. Sanchez Marcano*, Chemical engineering - modelling, simulation and similitude, Wiley VCH, 2007
[40] *O. Ioannidou and A. Zabaniotou*, "Agricultural residues as precursors for activated carbon production: A review", Renew. Sustain. Energ. Rev., **vol. 11**, 2007, pp. 1966-2005